Host defense mechanisms induce genome instability leading to rapid evolution in an opportunistic fungal pathogen

Amanda Smith*[1], Levi Morran[2], and Meleah A. Hickman[1,2]

* Corresponding author, ashurzi@emory.edu
[1] PhD program in Genetic and Molecular Biology, Emory University
[2] Department of Biology, Emory University

Key words: *Candida albicans*, *Caenorhabditis elegans*, fungal genomics, innate immunity, Reactive oxygen species, genetics

Abstract

The ability to generate genetic variation facilitates rapid adaptation in stressful environments. The opportunistic fungal pathogen *Candida albicans* frequently undergoes large-scale genomic changes, including aneuploidy and loss-of heterozygosity (LOH), following exposure to host environments. However, the specific host factors inducing *C. albicans* genome instability remain largely unknown. Here, we leveraged the genetic tractability of nematode hosts to investigate whether innate immune components, including antimicrobial peptides (AMPs) and reactive oxygen species (ROS), induced host-associated *C. albicans* genome instability. *C. albicans* associated with immunocompetent hosts carried multiple large-scale genomic changes including LOH, whole chromosome, and segmental aneuploidies. In contrast, *C. albicans* associated with immunocompromised hosts deficient in AMPs or ROS production had reduced LOH frequencies and fewer, if any, additional genomic changes. To evaluate if extensive host-induced genomic changes had long-term consequences for *C. albicans* adaptation, we experimentally evolved *C. albicans* in either immunocompetent or immunocompromised hosts and selected for increased virulence. *C. albicans* evolved in immunocompetent hosts rapidly increased virulence, but not in immunocompromised hosts. Taken together, this work suggests that host-produced ROS and AMPs induces genotypic plasticity in *C. albicans* which facilitates rapid evolution.

Introduction

62

63 The opportunistic fungal pathogen *Candida albicans* is typically commensal and
64 a component of the human microbiome (1). Yet, *C. albicans* is a leading cause of fungal
65 bloodstream infections and 40% of these infections result in mortality (2). In addition to
66 bloodstream infections, *C. albicans* causes non-lethal mucosal infections, including
67 vaginal and oral candidiasis (2). *C. albicans* infection is highly dependent on the host
68 context, including high estrogen levels (3), chronic stress (4), antibiotic use (5–7),
69 uncontrolled diabetes (8, 9), and immunosuppression (10, 11). In the absence of proper
70 immune recognition, fungal proliferation is uncontrolled, leading to infection. However
71 healthy individuals, despite having a fully functioning immune system, also experience
72 *C. albicans* infections. Infections primarily result from the commensal isolates becoming
73 pathogenic rather than an infection acquired from outside sources (12). The transition
74 from commensal to pathogenic may be facilitated by *C. albicans* phenotypic and
75 genotypic heterogeneity. *C. albicans* genetic diversity within and among individuals is
76 very high and often include numerous single nucleotide polymorphisms (SNPs) and loss
77 of heterozygosity (LOH) events (13). This genetic variation may be a direct
78 consequence of the stressors *C. albicans* encounters in the host which include immune
79 stressors and other microbes. Recent work has demonstrated the host environment
80 elevates *C. albicans* genome instability similar to *in vitro* stressors (14–18). However,
81 the specific host components that generate this instability are largely unknown.
82 Genomic variation is quite common in clinical *C. albicans* isolates (13, 19) and
83 includes polymorphisms, copy number variation, loss-of-heterozygosity (LOH), and
84 partial or whole chromosomal aneuploidies (19). This genomic variation indicates that

host environments either induce or maintain genetic variation in *C. albicans*. Murine infection models have found that when exposed to different host niches, *C. albicans* has a greater than 10-fold increase in LOH and frequent aneuploidy compared to *in vitr*o (14–16). Following host exposure, genomic changes generated in the murine environment often resulted in a more commensal-like phenotype and higher fitness inside the host (15, 16, 18, 20). However, the long-term genotypic and phenotypic consequences have not yet been extensively studied. *Caenorhabditis elegans* has also been used as a host model to assess *C. albicans* genome stability. *C. albicans* genome instability following *C. elegans* host association was detected across multiple *C. albicans* strains which resulted in changes to virulence (17). Together, murine and *C. elegans* models clearly demonstrate that host environments drive genetic diversity in *C. albicans* which cause phenotypic changes. However, it is remains unclear what specific host components contribute to *C. albicans* genome instability and how host-induced genome instability contributes to the long-term adaptability of *C. albicans*.

C. albicans encounters many different stressors within the host environment, including the immune system, which is designed to control and remove pathogens. The immune system recognizes *C. albicans* and other pathogens through pathogen recognition receptors (PRRs) that detect the specific microbial chemical signatures called pathogen-associated molecular patterns (PAMPs) (21). Recognition of pathogens like *C. albicans* triggers production of antimicrobial peptides (AMPs) which recruit phagocytic immune cells to the site of infection. Phagocytic immune cells produce reactive oxygen species (ROS) and reactive nitrogen species to control pathogen proliferation (22). Similar to humans, *C. elegans* produce ROS and AMPs in response to

pathogens. AMPs inhibit microbial growth through a variety of methods, including disrupting the cell membrane, and halting DNA, RNA, and protein synthesis (23). *C. elegans* AMP production is activated through a mitogen-activated protein kinase (MAPK) signaling cascade (24, 25) and includes SEK-1 (MAPKK), which is homologous to the mammalian MKK3/6 and MKK4 MAPKKs (26). Mutations in *C. elegans* SEK-1 increase host susceptibility to *C. albicans* and other microbial pathogens (26–29). Another conserved host defense mechanism is ROS production. Mammals produce ROS via five NADPH oxidases and two dual oxidases (30, 31) while *C. elegans* ROS production is mediated by a single dual oxidase BLI-3 in response to bacterial and fungal pathogens (29, 32–34). BLI-3 mutant hosts are more susceptible to *C. albicans* infection (35). ROS causes cellular toxicity through structural changes to the DNA (36) and generates double strand breaks in *C. albicans* (30). Together, host-produced AMPs and ROS act in various ways in order to inhibit *C. albicans* growth.

Here we investigated if host-produced AMPs and ROS induce *C. albicans* genome instability using the model host *C. elegans*. We infected wildtype and two different immunocompromised hosts with mutations in either *sek-1* (AMP production) or *bli-3* (ROS production) with *C. albicans* and measured the frequency and types of genome changes in *C. albicans*. Wildtype hosts elevate genome instability and generate greater genetic diversity in *C. albicans* compared to immunocompromised hosts. To evaluate the impact of greater genetic diversity in *C. albicans* driven by the host immune response, we evolved *C. albicans* virulence in both immunocompetent and immunocompromised hosts for ten passages. Within this relatively short *in vivo* experimental evolution, *C. albicans* rapidly increased virulence when evolved in

immunocompetent hosts but not when evolved in immunocompromised hosts. Taken together, our results suggest that host innate immune pathways are a source of genome instability in *C. albicans* and facilitate *C. albicans* adaptation.

Results

Host defense pathways elevate C. albicans genome instability

We and others, have shown that nematode and murine host environments induce *C. albicans* genome instability compared to *in vitro* (14–18), yet the specific host attributes driving genome instability have not been elucidated. Here, we tested whether components of host innate immune function drove host-associated genome instability by comparing *C. albicans* LOH between yeast extracted from immunocompetent and immunocompromised hosts (Fig. 1A). We used two different immunocompromised host genotypes, one carried a *sek-1* deletion and could not produce AMPs (31), the second host genotype carried a *bli*-3 deletion and could not produce ROS (29, 34). *C. albicans* LOH frequency was significantly reduced when extracted from *sek-1* and *bli-3* hosts compared to wildtype (N2) hosts (Figs. 1B, S1A&B) which implicates both *sek-1* and *bli-3* immune pathways as a source of pathogen genome instability.

Since *C. albicans* genetic background impacts mutation rates (16, 17), we also measured host-induced LOH frequency in a clinical *C. albicans* strain (37). Similar to the laboratory *C. albicans* strain, the clinical strain had a significantly reduced LOH frequency when extracted from *bli-3* hosts compared to wildtype hosts (Fig. 1C). Yet the

clinical *C. albicans* LOH frequency extracted from *sek-1* and wildtype hosts was not statistically different. However, *C. albicans* LOH frequency was notably higher in wildtype compared to *sek-1* hosts. Together, these data suggest that the *bli-3* pathway induces *C. albicans* genome instability regardless of pathogen genetic background, and the *sek-1* pathway may only contribute to genome instability in a strain-dependent manner.

In vitro and in vivo ROS elevate genome instability in cap1Δ/Δ C. albicans

In response to bacterial and fungal pathogens, *C. elegans* produces ROS via the BLI-3 dual oxidase (35). However, *C. albicans* has several mechanisms to combat ROS, including activation of antioxidant genes that detoxify ROS, whose expression is regulated by the Cap1p transcription factor (38, 39). To directly test whether *CAP1* protects *C. albicans* from ROS-induced genome instability, we compared *in vitro* LOH frequencies of wildtype and *cap1Δ/Δ C. albicans* strains exposed to 5 mM H_2O_2. Exposure to H_2O_2 elevated the LOH frequency in both wildtype and *cap1Δ/Δ C. albicans* strains. Yet, the increase in LOH was significantly higher in *cap1Δ/Δ* that had a 40-fold increase compared to wildtype that had a 15-fold increase (Fig. 2A & S2A). To assess whether *CAP1* mitigates *C. albicans* genome instability from host-produced ROS, we compared LOH frequencies between wildtype and *cap1Δ/Δ C. albicans* associated with immunocompetent and immunocompromised hosts. If host-produced ROS induces *C. albicans* genome instability, then *cap1Δ/Δ C. albicans* will have increased LOH in wildtype and *sek*-1 hosts that are capable of producing ROS, but not in *bli-3* hosts that

cannot. Compared to *in vitro*, all host environments increased *cap1*Δ/Δ LOH (Fig. S2B). Host-extracted *cap1*Δ/Δ LOH frequencies were higher compared to wildtype *C. albicans* for both wildtype and *sek-1* hosts, but not from *bli-3* hosts (Fig. 2B). Together, these data demonstrate that host-produced ROS elevated *C. albicans* genome instability. Additionally, cap1p-mediated ROS detoxification is important for mitigating ROS-induced *C. albicans* genome instability both *in vitro* and *in vivo*.

Endogenous and exogenous antioxidants break down ROS through a variety of mechanisms. We next wanted to determine whether antioxidants mitigate *C. albicans* genome instability resulting from host-produced ROS. We compared host-associated *C. albicans* LOH in the presence or absence of 25 μM of lipoic acid, an antioxidant involved in the breakdown of ROS (34). In the presence of lipoic acid, host-associated *C. albicans* LOH was significantly reduced when extracted from wildtype and *sek-1* hosts (Figs. 2C & S2C). In contrast, lipoic acid did not decrease *C. albicans* LOH when extracted from *bli-3* hosts, (Figs. 2C & S2C). This suggests that antioxidants are effective in reducing *C. albicans* genome instability in ROS-producing hosts. Together, these data suggest that both *in vitro* and *in vivo* ROS elevates genome instability in a *cap1*Δ/Δ mutant, and that *C. albicans* genome instability caused by host-produced ROS can be alleviated with the addition of antioxidants.

Host-produced AMPs and ROS cause aneuploidy and abundant LOH events in C. albicans

LOH assays are an easy, useful and established way to measure *C. albicans* genome instability (40, 41), however, they are limited to measuring a heterozygous marker at a single genomic location. To characterize whether host immunity drives other genomic alterations, we whole-genome sequenced single colony isolates associated with wildtype, *sek-1* and *bli-3* hosts that were isolated either on media that selected for LOH events (2-DOG; Fig. 3A) or media that did not select for LOH events (YPD; Fig. S3). Among LOH-selected isolates extracted from wildtype hosts, *GAL1* LOH on Chr1 was mediated via break-induced recombination (4/6) or via whole chromosome loss and reduplication (1/6). For the break-induced recombination LOH events, there was no evidence for a common breakpoint or recombination hotspot mediating host-induced *GAL1* LOH. Additional large-tract LOH events (42, 43), homozygous from the site of the DNA break to the end of the chromosome, and whole-chromosomal, and segmental aneuploidies were identified in 5/6 LOH-selected isolates from wildtype hosts (Fig. 3A). However, no aneuploidy was detected in *C. albicans* from immunocompromised host backgrounds (Fig. 3A). Four isolates carried a long-tract LOH or segmental aneuploidy on Chr2 with breakpoints ranging between positions 1,795,723 and 2,155,170; four carried a 170 kb LOH tract or segmental aneuploidy on Chr6, whose breakpoint corresponds with position 861,044, the beginning of a major repeat sequence (MRS). One isolate was trisomic for Chr7 and tetrasomic for Chr6. Even among non-LOH selected isolates associated with wildtype hosts, 50% had undergone whole-chromosome LOH on Chr2 (Fig. S3). But no large-scale genomic changes were detected in non-LOH selected isolates associated with *sek-1* hosts (Fig. S3A). Thus,

immune components in wildtype hosts induced large-scale genomic changes in *C. albicans*.

C. albicans evolves rapidly in immunocompetent, but not immunocompromised hosts

Thus far, our results support a model that innate immunity generates *C. albicans* genetic variation by inducing genome instability. As genetic variation is a fundamental requirement for a response to natural selection, we hypothesized that *C. albicans* would evolve more rapidly in immunocompetent hosts, as compared to immunocompromised hosts. To test this hypothesis, were performed *in vivo* experimental evolution utilizing immunocompetent and immunocompromised hosts and selected for increased *C. albicans* virulence. Given that exposure to both *bli-3* and *sek-1* hosts reduced genome-wide genetic diversity in *C. albicans* (Fig. 3), we selected AU-37 (glp-4; sek-1) as our immunocompromised hosts for logistical purposes (see methods). We infected six parallel populations of 50 hosts for both immunocompetent and immunocompromised hosts. When a host population reached 50% death, we extracted *C. albicans* from the dead hosts to infect a new host population, selecting for *C. albicans* associated with early host death (Fig. 4A). We evolved *C. albicans* in this manner for a total of ten passages (Fig. 4A). After five passages in immunocompetent hosts, the average time to 50% death was ~8 days which was significantly lower than the initial passage with an average of 12 days (Fig. 4B), indicating increased virulence in *C. albicans*. This increased virulence was subsequently maintained throughout the remainder of the evolution experiment (Fig. 4B). In contrast, there was no change in the average time to

50% death in immunocompromised hosts throughout ten passages, despite being more susceptible initially to *C. albicans* infection compared to immunocompetent hosts, (Fig. 4C). Therefore, *C. albicans* did not respond to selection for increased virulence in the immunocompromised hosts within ten passages. Together, these results support our hypothesis that host immunity-induced genomic changes generated in *C. albicans* populations facilitated a strong response to this selection regime.

To validate that increased virulence observed from immunocompetent hosts was a direct result of our selection pressure and not the passaging itself, we passaged *C. albicans* in parallel experimental conditions but in the absence of hosts. We then infected immunocompetent and immunocompromised hosts with the 'no-host' evolved (grey, P10) *C. albicans* and found that 'no-host' evolved *C. albicans* did not exhibit changes in virulence relative to the ancestral (P0) state, regardless of host immune status (Fig. 4D). Thus, selection for virulence was responsible for the increase in virulence in *C. albicans* evolved in immunocompetent hosts.

Discussion

We previously reported that healthy, immunocompetent hosts induce *C. albicans* genome instability. We followed this up by investigating whether host innate immune pathways drive pathogen genome instability(17). By using wildtype and two immunocompromised hosts deficient for AMP production (*sek-1*) and ROS production (*bli-3*), we compared the differences in host-associated *C. albicans* genome stability and mutational landscape. *C. albicans* associated with either immunocompromised host had

reduced relative LOH frequencies compared to those associated with wildtype hosts (Figure 1). Similar to several other host passaging experiments and whole-genome sequencing results from clinical isolates (14, 16, 19), many of our isolates extracted from wildtype hosts contained large-scale genomic changes including whole and segmental chromosomal aneuploidy and/or additional LOH events (Figure 3). We detected the presence of an extra copies of Chr6 following host exposure, consistent with previous observations of host-induced genomic alterations that used a murine OPC infection model (14). The aforementioned study suggested Chr6 aneuploidy produces more commensal-like phenotypes inside the host environment. Whether this occurred in our isolate with chr6 aneuploidy following host exposure has yet to be investigated. We also detected an extra copy of Chr7 in one isolate following wildtype host exposure. In a gastrointestinal (GI) murine model of candidiasis, Chr7 trisomy results in higher *C. albicans* fitness within the GI tract compared to the euploid strain (16). Therefore, specific aneuploidies may enable host adaptation. Following immunocompromised (*sek-1* or *bli-3*) host-associated, *C. albicans* isolates did not carry any detectable aneuploidy and only a small number (2/8) had an LOH event that was not selected for (Figure 2). These results suggest that both AMPs and ROS act as stressors on *C. albicans* that enable the generation of genetic variation which might lead to phenotypic changes that create a more commensal host–pathogen relationship.

The host has a variety of mechanisms capable of controlling microbial growth. Because *C. albicans* is normally, it must strike a delicate balance with the host to evade detection. Overgrowth of *C. albicans* initiates an immune response that initially includes the production of AMPs. AMPs then recruit phagocytes to the site of infection which

produce ROS (22). We found that the removal of host-produced AMPs and ROS decrease LOH frequency in *C. albicans* and overall genomic changes compared to *C. albicans* extracted from wildtype hosts (Figures 1 & 3). We only found a significant decrease in the relative LOH frequency in both the laboratory and bloodstream *C. albicans* extracted from *bli-3* hosts compared to wildtype hosts. However, we did not detect a significant decrease the relative LOH frequency in the bloodstream strain extracted from *sek-1* hosts (Figs 1B&C). This suggests that host-produced ROS generates genome instability regardless of pathogen background. However, the *sek-1* pathway may only produce AMPs in response to certain strains of *C. albicans*. We propose that the differences observed in genome instability between different strains of *C. albicans* is potentially due to recognition of different PAMPs by host PRR which can trigger different immune responses (46).

Because host-produced ROS represented a conserved source of genome instability across two different strains of *C. albicans*, we further investigated the role of host-produced ROS in generating genome instability. *C. albicans* has several mechanisms for detoxify ROS, one of which is regulated by the transcription factor Cap1p. *Cap1Δ/Δ* mutants are more susceptible to *in vitro* ROS killing (38, 47). Here we show that *cap1Δ/Δ C. albicans* genome instability was increased compared to wildtype *C. albicans* in hosts capable of producing ROS (N2 and *sek-1*) but not in *bli-3* hosts incapable of producing ROS (Fig. 2B). These findings suggest that host-produced ROS through the bli-3 dual-oxidase induces genome instability in *C. albicans* and that Cap1p is important for detoxification of host-produced ROS. Recent work in *E. coli*, demonstrated that when exposed to low levels of ROS, *E. coli* exhibits a priming

response in which evolution in ROS occurs faster and cells develop greater resistance as opposed to non-primed cells (48). Our results suggest that host-produced ROS might be priming *C. albicans* allowing for tolerance of greater stress.

Although counterintuitive, LOH increases genetic diversity by unmasking recessive alleles, leading to phenotypic changes (43). For example, LOH of drug-resistant alleles of *ERG11*, *TAC1* or *MRR1* increases antifungal drug resistance (49–51). Similarly, aneuploidy offers a short-term solution that organisms use during adaptation (52–54) and have been shown to be advantages under certain conditions including the host environment(14–16). Because we detected large-scale LOH events and aneuploidy in isolates exposed to immunocompetent hosts, we suggest that these genetic changes facilitate rapid adaptation to the host. Through experimental evolution in immunocompetent and immunocompromised *C. elegans* hosts, we found that *C. albicans* evolved increased virulence rapidly in immunocompetent hosts, but not in immunocompromised hosts (Figure 4). Our work identifies AMPs and ROS as important conserved innate immune responses that generate genome instability in the fungal pathogen, *C. albicans*. We propose that the generation of genetic variation in response to host-produce ROS and AMPs represents a way in which *C. albicans* can quickly respond to host stressors thus further tolerating these stressors or avoiding further immune attack. Finally, we demonstrate that immunocompetent hosts facilitate rapid evolution under selection for increased virulence. We hypothesize this is a result from the combination of strong selective pressure and the greater genetic variation generated in *C. albicans* by the innate immune response. Therefore, the host environment can significantly alter the evolutionary trajectories of *C. albicans* populations. While many

336 factors may contribute to the shift from commensal to pathogen in *C. albicans*
337 populations, it is clear that the host immune system can determine the level of genetic
338 variation available for a response to selection. Thus, identifying the selective pressures
339 that drive the shift from commensal to pathogen are critical for understanding *C.*
340 *albicans* evolution within hosts.
341
342
343 **Methods**
344
345 *Strains and Maintenance*
346 *C. albicans* and *C. elegans* strains for this study are listed in Table S1. Yeast
347 strains (55–57) were stored at -80°C and maintained on YPD (yeast peptone dextrose;
348 1% yeast extract, 2% bactopeptone, 2% glucose, 0.004% adenine, 0.008% uridine) at
349 30°C. Strains were initially struck onto YPD agar plates from frozen glycerol stocks and
350 incubated at 30°C for 48 hours and single colonies used as the “parental strain” in
351 subsequent in vivo experiments. Nematode populations were maintained on plates
352 containing nematode growth media (NGM) with *E. coli* (OP50) for a food source. *C.*
353 *elegans* were transferred to a new plate containing freshly seeded *E. coli* every three to
354 four days. For genome stability assays, treatment plates were seeded with both *C.*
355 *albicans* and *E. coli* and supplemented with 0.2 g/L streptomycin to inhibit overgrowth of
356 *E. coli*. For fecundity and genome stability assays, NGM was supplemented with
357 0.08g/L of uridine and 0.08g/L of histidine to facilitate growth of auxotrophic *C. albicans*
358 strains.

359

360 *Host-associated C. albicans genome stability*

361 *Host preparation:* NGM plates are seeded with a mixture of *E. coli* and *C.*
362 *albicans* 24 h prior to host preparation. To seed plates, single colonies of *C. albicans*
363 were inoculated into 3 mL YPD and incubated overnight at 30°C. Cultures were
364 adjusted with ddH_2O to a final concentration of 3.0 OD_{600} per mL. Simultaneously, a
365 single colony of *E. coli* was inoculated into 50 mL LB and incubated for 24-48 h at 30°C.
366 The *E. coli* culture was pelleted and washed twice with 1 mL ddH_2O. The pellet was
367 weighed and diluted to final concentration of 200 mg/mL. For *in vitro* treatments, 250 µL
368 *C. albicans* was spread onto NGM + streptomycin agar plates and incubated overnight
369 at 30°C. For *in vivo* treatment plates, 6.25 µL *C. albicans*, 31.25 µL *E. coli*, and brought
370 to a final volume of 250 µL with ddH_2O, was spread onto NGM + streptomycin agar
371 plates and incubated overnight at 30°C. For experimental evolution experiments, *C.*
372 *albicans* treatment plates had 1.25 µL of *C. albicans* and 6.25 µL of *E. coli* and were
373 brought to a final volume of 50 µL. The entire 50 µL was spotted onto the center of a 35-
374 mm-diameter NGM plus streptomycin agar plate, followed by incubation at room
375 temperature overnight before the addition of eggs or transferred nematodes.

376 To synchronize *C. elegans* populations, nematodes and eggs were washed off
377 plates with M9 buffer, transferred to 15 mL conical tubes, and pelleted via centrifugation
378 (2 min at 1200 rpm). The pellet was resuspended in 2 mL of 25% bleach, mixed via
379 inversion for 2 min, and centrifuged for 2 min at 1200 rpm. The pellet was washed twice
380 with 3 mL ddH_2O and resuspended with 1 mL ddH_2O. To determine the concentration of
381 eggs, 10 µL was pipetted onto a concave slide, eggs were visualized microscopely and

counted, and the suspension was adjusted to a concentration of ~100 eggs per 100 µL with M9.

Host-associated yeast extractions: Yeast extractions were performed as described previously (17). Hosts exposed to *C. albicans* were washed from plates with 3 mL M9 and pelleted via centrifugation (2 min at 2,000 RPM). The supernatant was removed and the pellet was resuspended with 1 mL 3% bleach, transferred to a microcentrifuge tube, and incubated for three minutes and subsequently centrifuged for 1 min at 12,000 rpm. The supernatant was removed and washed with 1 mL of M9 and centrifuged for one minute at 12,000 rpm. The wash was repeated two more times to ensure all bleach was removed. 100 µl aliquots of nematode suspension were transferred to 0.6 mL clear microtubes for manual disruption with a motorized pestle. After one minute of manual disruption, the worm intestine solution was then diluted accordingly with an M9 buffer and plated on YPD + 0.034mg/L chloramphenicol to prevent any bacterial colonies from arising.

GAL1 Loss of Heterozygosity assay

In vitro: Single colonies of *C. albicans* were inoculated in 3 mL YPD grown overnight at 30°C and subsequently diluted to 3 OD in ddH_2O. 250 µL was plated and spread onto NGM + streptomycin plates and incubated overnight at 30°C and transferred to 20°C for four days to mimic the conditions of the *in vivo* LOH assay. On day four, yeast cells were washed off with ddH_2O, harvested by centrifugation, washed once with ddH_2O, resuspended in 1 mL of ddH_2O and serially diluted for single colony

405 growth. To determine the total cell viability, 100 µL of 10^{-6} dilution was plated onto YPD
406 and grown for 48 h at 30°C. To identify cells that lost *GAL1*, 100 µL of 10^{-2} and 10^{-3}
407 dilution was plated onto 2-deoxygalactose (2-DOG; 0.17% yeast nitrogen base without
408 amino acids 0.5% ammonium sulfate, 0.0004% uridine, 0.0004% histidine, 0.1% 2-
409 deoxygalacose, 3% glycerol) and colony forming units (CFUs) counted following 72
410 hours incubation at 30°C. LOH assays performed with α-Lipoic acid were performed as
411 described above but α-Lipoic acid (Sigma-Aldrich #1077-28-7) was dissolved in 100%
412 ethanol and added to NGM media containing 0.2 g/L streptomycin sulfate to a final
413 concentration of 25 µM.
414 *In vivo:* The approach was very similar as the *in vitro* LOH assay described
415 above, with the following changes. A population of ~100 nematodes were plated on
416 each treatment plate containing both *C. albicans* and *E. coli.* On day four, yeast were
417 extracted as described in the previous section. A dilution of 10^{-1} and 10^{-2} was plated on
418 YPD + chloramphenicol to enumerate total growth and undiluted cells were plated on 2-
419 DOG to select for the loss of *GAL1.* Three technical replicates were used for each *C.*
420 *albicans* strain for both *in vitro* and *in vivo* experiments. At least three biological
421 replicates were used for each genome stability assay.
422
423 *Hydrogen Peroxide Exposure and Genome Stability:*
424 Six single colonies of *C. albicans* were inoculated in either 2 ml of YPD or in 2
425 mL of YPD containing 5 mM H_2O_2, grown for 20 h at 30°C. Cultures were centrifuged at
426 2000 rpm for 2 minutes. The supernatant was removed, and the pellet was washed

once with 1 mL of ddH_2O. Cultures were serially diluted for single colony growth. Loss-of-heterozygosity assays were performed to determine the frequency of LOH.

Whole genome sequencing and analysis

Genomic DNA was isolated with phenol chloroform as described previously (58). Whole genome sequencing was performed through the Microbial Genome Sequencing Center using a single library preparation method based on the Illumina Nextera kit. Libraries were sequencing using paired end (2 x 150 bp) reads on the NextSeq 550 platform. Adaptor sequences and low-quality reads were trimmed using Trimmomatic (v0.39 LEADING:3 TRAILING: 3 SLIDINGWINDOW: 4:15 MINLEN: 36 TOPHRED33) (59). All reads were mapped to the phased *C. albicans* reference genome using the haplotypo python script 'mapping.py'. This tool uses the Burrows-Wheeler Aligner MEM (BWA v0.1.19) algorithm to align the sequencing reads to the reference genome followed by Samtools (v0.1.19) to sort, mark duplicates, and create a BAM file. The average coverage and read depth for each isolate we calculated using samtools 'coverage' (Supplemental File 1). Variant files were created using the haplotypo python script 'var_calling.py' using the BCFtools calling method with a minimum coverage of 30. Variants were filtered using the following parameters "DP<=30 || QD < 2.0 || MQ < 40.0 || FS > 60.0 || MQRankSum < -12.5 || ReadPosRankSum < -8.0 Identification of aneuploidy, CNVs, and LOH were conducted using whole genome sequencing data and the Yeast Mapping Analysis Pipeline (YMAP). BAM files were uploaded to YMAP and plotted using the Candida albicans reference genome (A21-s02smo8-r09) with corrections for chromosome end bias and GC content (60).

450 *Experimental Evolution*

451 Wildtype SC5314 *C. albicans* was evolved in immunocompetent (glp-4) and
452 immunocompromised (glp-4; sek-1) nematode host backgrounds. We chose to use the
453 glp-4 background because of the temperature sensitive sterility mutation. At 25 °C, the
454 glp-4 nematodes are unable to reproduce allowing us to track the survival of a single
455 generation of nematodes (45). Additionally, we chose to use the *sek-1* background for
456 our immunocompromised host because of the availability of *sek-1* and glp-4 mutations
457 in the same background. This allows for complete control over tracking the same
458 population of 50 worms for each passage, which was required for our selection regime.
459 For each host background, experimental evolution was performed with six replicate
460 evolved lines. NGM plates were seeded with *C. albicans* and *E. coli* 24 h prior to the
461 start of the evolution. On Day 1, nematodes were synchronized and incubated at 25°C
462 for 48 h. On Day 3, 50-L4 nematodes were transferred to a newly seeded NGM plate
463 containing both *C. albicans* and *E. coli*. Every day the host population was monitored for
464 survival and dead nematodes were transferred to a 1.5 mL microcentrifuge tube
465 containing 500 µL M9 buffer. Every other day, the remaining live nematodes were
466 transferred to newly seeded plates to replenish their food supply. Once the host
467 population reached 50% mortality, *C. albicans* was extracted from only the 25 dead
468 nematodes by centrifuging the 1.5mL microcentrifuge tube for 30 seconds at maximum
469 speed. The supernatant was removed and 500 uL of 3% bleach was added for 2 min. to
470 kill any microbes on the nematode surfaces and centrifuged for 30s at maximum speed.
471 The supernatant was removed and the nematode pellet was washed three times with
472 500 uL M9. The nematodes were manual disrupted using a motorized pestle for one

minute and all the intestinal extracts were inoculated into 2 mL YPD containing 0.034mg/L chloramphenicol to prevent any bacterial growth. This inoculum was used to seed a new population of 50 hosts in the subsequent passage.

Statistical analysis:

Statistical analysis was performed using GraphPad Prism 8 software. Data sets were tested for normality using the D'Agnostino & Pearson omnibus normality test.

Acknowledgments/Author Contributions:

We would like to thank Eduardo Scopel Ferreira Da Costa (University of Georgia), Abdul-Rhanman Adamu Bukari (University of Manitoba), and Venkat Talla (Emory University) for helpful discussions regarding sequencing analysis. We would also like to thank Ognenka Avramovska for thoughtful conversations and critical reading of the manuscript. This research is supported by NSF DEB-1943415 (MAH), NSF DEB-1750553 (LTM), and Emory University startup funds (MAH).

ACS and MAH designed the study. ACS conducted all of the experiments. ACS and MAH analyzed the data. ACS, LTM, and MAH wrote, reviewed and edited the manuscript.

Data Availability:

All supplemental files and relevant data will be posted on the Dryad Digital Repository, pending manuscript acceptance. Raw sequencing reads will be deposited NCBI sequence read archive pending manuscript acceptance.

References

1. Perlroth J, Choi B, Spellberg B. 2007. Nosocomial fungal infections: epidemiology, diagnosis, and treatment. Med Mycol 45:321–346.

2. Pfaller MA, Diekema DJ. 2007. Epidemiology of Invasive Candidiasis: a Persistent Public Health Problem. Clin Microbiol Rev 20:133–163.

3. Sobel JD. 2007. Vulvovaginal candidosis. Lancet 369:1961–1971.

4. Akimoto-Gunther L, Bonfim-Mendonça P de S, Takahachi G, Irie MMT, Miyamoto S, Consolaro MEL, Svidzinsk TIE. 2016. Highlights Regarding Host Predisposing Factors to Recurrent Vulvovaginal Candidiasis: Chronic Stress and Reduced Antioxidant Capacity. Plos One 11:e0158870.

5. Ahmad A, Khan AU. 2009. Prevalence of Candida species and potential risk factors for vulvovaginal candidiasis in Aligarh, India. Eur J Obstet Gyn R B 144:68–71.

6. Grigoriou O, Baka S, Makrakis E, Hassiakos D, Kapparos G, Kouskouni E. 2006. Prevalence of clinical vaginal candidiasis in a university hospital and possible risk factors. Eur J Obstet Gyn R B 126:121–125.

7. Gonçalves B, Ferreira C, Alves CT, Henriques M, Azeredo J, Silva S. 2015. Vulvovaginal candidiasis: Epidemiology, microbiology and risk factors. Crit Rev Microbiol 42:1–23.

8. Gunther LSA, Martins HPR, Gimenes F, Abreu ALP de, Consolaro MEL, Svidzinski TIE. 2014. Prevalence of Candida albicans and non-albicans isolates from vaginal secretions: comparative evaluation of colonization, vaginal candidiasis and recurrent vaginal candidiasis in diabetic and non-diabetic women. Sao Paulo Med J 132:116–120.

9. Leon EM de, Jacober SJ, Sobel JD, Foxman B. 2002. Prevalence and risk factors for vaginal Candidacolonization in women with type 1 and type 2 diabetes. Bmc Infect Dis 2:1.

10. Iliev ID, Leonardi I. 2017. Fungal dysbiosis: immunity and interactions at mucosal barriers. Nat Rev Immunol 17:635–646.

526 11. Underhill DM, Iliev ID. 2014. The mycobiota: interactions between commensal fungi and the
527 host immune system. Nat Rev Immunol 14:nri3684.

528 12. Nucci M, Anaissie E. 2001. Revisiting the Source of Candidemia: Skin or Gut? Clin Infect
529 Dis 33:1959–1967.

530 13. Sitterlé E, Maufrais C, Sertour N, Palayret M, d'Enfert C, Bougnoux M-E. 2019. Within-
531 Host Genomic Diversity of Candida albicans in Healthy Carriers. Sci Rep-uk 9:2563.

532 14. Forche A, Cromie G, Gerstein AC, Solis NV, Pisithkul T, Srifa W, Jeffery E, Abbey D, Filler
533 SG, Dudley AM, Berman J. 2018. Rapid Phenotypic and Genotypic Diversification After
534 Exposure to the Oral Host Niche inCandida albicans. Genetics genetics.301019.2018.

535 15. Forche A, Solis NV, Swidergall M, Thomas R, Guyer A, Beach A, Cromie GA, Le GT,
536 Lowell E, Pavelka N, Berman J, Dudley AM, Selmecki A, Filler SG. 2019. Selection of Candida
537 albicans trisomy during oropharyngeal infection results in a commensal-like phenotype. Plos
538 Genet 15:e1008137.

539 16. Ene IV, Farrer RA, Hirakawa MP, Agwamba K, Cuomo CA, Bennett RJ. 2018. Global
540 analysis of mutations driving microevolution of a heterozygous diploid fungal pathogen. Proc
541 National Acad Sci 115:201806002.

542 17. Smith AC, Hickman MA. 2020. Host-Induced Genome Instability Rapidly Generates
543 Phenotypic Variation across Candida albicans Strains and Ploidy States. Msphere 5:e00433-20.

544 18. Forche A, Magee PT, Selmecki A, Berman J, May G. 2009. Evolution in Candida albicans
545 populations during a single passage through a mouse host. Genetics 182:799–811.

546 19. Hirakawa MP, Martinez DA, Sakthikumar S, Anderson MZ, Berlin A, Gujja S, Zeng Q,
547 Zisson E, Wang JM, Greenberg JM, Berman J, Bennett RJ, Cuomo CA. 2014. Genetic and
548 phenotypic intra-species variation in Candida albicans. Genome Res 25:413–25.

549 20. Tso GHW, Reales-Calderon JA, Tan ASM, Sem X, Le GTT, Tan TG, Lai GC, Srinivasan
550 KG, Yurieva M, Liao W, Poidinger M, Zolezzi F, Rancati G, Pavelka N. 2018. Experimental
551 evolution of a fungal pathogen into a gut symbiont. Science 362:589–595.

552 21. Akira S, Uematsu S, Takeuchi O. 2006. Pathogen Recognition and Innate Immunity. Cell
553 124:783–801.

554 22. Netea MG, Brown GD, Kullberg BJ, Gow NAR. 2008. An integrated model of the
555 recognition of Candida albicans by the innate immune system. Nat Rev Microbiol 6:67–78.

556 23. Shai Y. 2002. Mode of action of membrane active antimicrobial peptides. Peptide Sci
557 66:236–248.

558 24. Kim DH, Ausubel FM. 2005. Evolutionary perspectives on innate immunity from the study
559 of Caenorhabditis elegans. Curr Opin Immunol 17:4–10.

560 25. Kim DH, Feinbaum R, Alloing G, Emerson FE, Garsin DA, Inoue H, Tanaka-Hino M,
561 Hisamoto N, Matsumoto K, Tan M-W, Ausubel FM. 2002. A Conserved p38 MAP Kinase
562 Pathway in *Caenorhabditis elegans* Innate Immunity. Science 297:623–626.

563 26. Tanaka-Hino M, Sagasti A, Hisamoto N, Kawasaki M, Nakano S, Ninomiya-Tsuji J,
564 Bargmann CI, Matsumoto K. 2002. SEK-1 MAPKK mediates Ca2+ signaling to determine
565 neuronal asymmetric development in Caenorhabditis elegans. Embo Rep 3:56–62.

566 27. Feistel DJ, Elmostafa R, Nguyen N, Penley M, Morran L, Hickman MA. 2019. A Novel
567 Virulence Phenotype Rapidly Assesses Candida Fungal Pathogenesis in Healthy and
568 Immunocompromised Caenorhabditis elegans Hosts. Msphere 4.

569 28. Feistel DJ, Elmostafa R, Hickman MA. 2020. Virulence phenotypes result from interactions
570 between pathogen ploidy and genetic background. Ecol Evol 10:9326–9338.

571 29. Hoeven R van der, McCallum KC, Cruz MR, Garsin DA. 2011. Ce-Duox1/BLI-3 Generated
572 Reactive Oxygen Species Trigger Protective SKN-1 Activity via p38 MAPK Signaling during
573 Infection in C. elegans. Plos Pathog 7:e1002453.

574 30. Thomson GJ, Hernon C, Austriaco N, Shapiro RS, Belenky P, Bennett RJ. 2019.
575 Metabolism-induced oxidative stress and DNA damage selectively trigger genome instability in
576 polyploid fungal cells. Embo J 38:e101597.

577 31. Irazoqui JE, Urbach JM, Ausubel FM. 2010. Evolution of host innate defence: insights from
578 Caenorhabditis elegans and primitive invertebrates. Nat Rev Immunol 10:47–58.

579 32. Moribe H, Konakawa R, Koga D, Ushiki T, Nakamura K, Mekada E. 2012. Tetraspanin Is
580 Required for Generation of Reactive Oxygen Species by the Dual Oxidase System in
581 Caenorhabditis elegans. Plos Genet 8:e1002957.

582 33. Hoeven R van der, Cruz MR, Chávez V, Garsin DA. 2015. Localization of the Dual Oxidase
583 BLI-3 and Characterization of Its NADPH Oxidase Domain during Infection of Caenorhabditis
584 elegans. Plos One 10:e0124091.

585 34. Chávez V, Mohri-Shiomi A, Garsin DA. 2009. Ce-Duox1/BLI-3 Generates Reactive Oxygen
586 Species as a Protective Innate Immune Mechanism in Caenorhabditis elegans ▿ . Infect Immun
587 77:4983–4989.

588 35. Jain C, Pastor K, Gonzalez AY, Lorenz MC, Rao RP. 2013. The role of Candida albicans
589 AP-1 protein against host derived ROS in in vivo models of infection. Virulence 4:67–76.

590 36. Jena NR. 2012. DNA damage by reactive species: Mechanisms, mutation and repair. J
591 Biosciences 37:503–517.

592 37. Marr KA, White TC, Burik JH van, Bowden RA. 1997. Development of Fluconazole
593 Resistance in Candida albicans Causing Disseminated Infection in a Patient Undergoing Marrow
594 Transplantation. Clin Infect Dis 25:908–910.

595 38. Alarco A-M, Raymond M. 1999. The bZip Transcription Factor Cap1p Is Involved in
596 Multidrug Resistance and Oxidative Stress Response inCandida albicans. J Bacteriol 181:700–
597 708.

598 39. Dantas A da S, Day A, Ikeh M, Kos I, Achan B, Quinn J. 2015. Oxidative Stress Responses
599 in the Human Fungal Pathogen, Candida albicans. Biomol 5:142–165.

600 40. Forche A, May G, Magee PT. 2005. Demonstration of Loss of Heterozygosity by Single-
601 Nucleotide Polymorphism Microarray Analysis and Alterations in Strain Morphology in Candida
602 albicans Strains during Infection. Eukaryot Cell 4:156–165.

603 41. Forche A, Abbey D, Pisithkul T, Weinzierl MA, Ringstrom T, Bruck D, Petersen K, Berman
604 J. 2011. Stress Alters Rates and Types of Loss of Heterozygosity in Candida albicans. Mbio
605 2:e00129-11.

606 42. Llorente B, Smith CE, Symington LS. 2008. Break-induced replication: What is it and what
607 is it for? Cell Cycle 7:859–864.

608 43. Feri A, Loll-Krippleber R, Commere P-H, Maufrais C, Sertour N, Schwartz K, Sherlock G,
609 Bougnoux M-E, d'Enfert C, Legrand M. 2016. Analysis of Repair Mechanisms following an
610 Induced Double-Strand Break Uncovers Recessive Deleterious Alleles in the Candida albicans
611 Diploid Genome. Mbio 7:e01109-16.

612 44. Kino K, Sugiyama H. 2001. Possible cause of G·C→C·G transversion mutation by guanine
613 oxidation product, imidazolone. Chem Biol 8:369–378.

614 45. Rastogi S, Borgo B, Pazdernik N, Fox P, Mardis ER, Kohara Y, Havranek J, Schedl T. 2015.
615 Caenorhabditis elegans glp-4 Encodes a Valyl Aminoacyl tRNA Synthetase. G3 Genes Genomes
616 Genetics 5:2719–2728.

617 46. Zheng N-X, Wang Y, Hu D-D, Yan L, Jiang Y-Y. 2015. The role of pattern recognition
618 receptors in the innate recognition of Candida albicans. Virulence 6:347–361.

619 47. Enjalbert B, Smith DA, Cornell MJ, Alam I, Nicholls S, Brown AJP, Quinn J. 2006. Role of
620 the Hog1 Stress-activated Protein Kinase in the Global Transcriptional Response to Stress in the
621 Fungal Pathogen Candida albicans. Mol Biol Cell 17:1018–1032.

622 48. Rodríguez-Rojas A, Kim JJ, Johnston P, Makarova O, Eravci M, Weise C, Hengge R, Rolff
623 J. 2020. Non-lethal exposure to H2O2 boosts bacterial survival and evolvability against oxidative
624 stress. Plos Genet 16:e1008649.

625 49. White TC. 1997. The presence of an R467K amino acid substitution and loss of allelic
626 variation correlate with an azole-resistant lanosterol 14alpha demethylase in Candida albicans.
627 Antimicrob Agents Ch 41:1488–1494.

628 50. Dunkel N, Blaß J, Rogers PD, Morschhäuser J. 2008. Mutations in the multi-drug resistance
629 regulator MRR1, followed by loss of heterozygosity, are the main cause of MDR1
630 overexpression in fluconazole-resistant Candida albicans strains. Mol Microbiol 69:827–840.

631 51. Coste A, Turner V, Ischer F, Morschhäuser J, Forche A, Selmecki A, Berman J, Bille J,
632 Sanglard D. 2006. A Mutation in Tac1p, a Transcription Factor Regulating CDR1 and CDR2, Is
633 Coupled With Loss of Heterozygosity at Chromosome 5 to Mediate Antifungal Resistance in
634 Candida albicans. Genetics 172:2139–2156.

635 52. Rancati G, Pavelka N, Fleharty B, Noll A, Trimble R, Walton K, Perera A, Staehling-
636 Hampton K, Seidel CW, Li R. 2008. Aneuploidy Underlies Rapid Adaptive Evolution of Yeast
637 Cells Deprived of a Conserved Cytokinesis Motor. Cell 135:879–893.

638 53. Yona AH, Manor YS, Herbst RH, Romano GH, Mitchell A, Kupiec M, Pilpel Y, Dahan O.
639 2012. Chromosomal duplication is a transient evolutionary solution to stress. Proc National Acad
640 Sci 109:21010–21015.

641 54. Pavelka N, Rancati G, Zhu J, Bradford WD, Saraf A, Florens L, Sanderson BW, Hattem GL,
642 Li R. 2010. Aneuploidy confers quantitative proteome changes and phenotypic variation in
643 budding yeast. Nature 468:321–325.

644 55. Gillum AM, Tsay EYH, Kirsch DR. 1984. Isolation of the Candida albicans gene for
645 orotidine-5′-phosphate decarboxylase by complementation of S. cerevisiae ura3 and E. coli pyrF
646 mutations. Mol Gen Genetics Mgg 198:179–182.

647 56. Hickman MA, Zeng G, Forche A, Hirakawa MP, Abbey D, Harrison BD, Wang Y-M, Su C,
648 Bennett RJ, Wang Y, Berman J. 2013. The 'obligate diploid' Candida albicans forms mating-
649 competent haploids. Nature 494:55.

650 57. Noble SM, French S, Kohn LA, Chen V, Johnson AD. 2010. Systematic screens of a
651 Candida albicans homozygous deletion library decouple morphogenetic switching and
652 pathogenicity. Nat Genet 42:590–598.

653 58. Selmecki A, Forche A, Berman J. 2006. Aneuploidy and Isochromosome Formation in Drug-
654 Resistant Candida albicans. Science 313:367–370.

655 59. Bolger AM, Lohse M, Usadel B. 2014. Trimmomatic: a flexible trimmer for Illumina
656 sequence data. Bioinformatics 30:2114–2120.

657 60. Abbey DA, Funt J, Lurie-Weinberger MN, Thompson DA, Regev A, Myers CL, Berman J.
658 2014. YMAP: a pipeline for visualization of copy number variation and loss of heterozygosity in
659 eukaryotic pathogens. Genome Med 6:100.

Figure Legends:

Figure 1: Host immunity impacts *C. albicans* genome stability
A) Experimental overview of in vivo experiments. **B)** Laboratory *C. albicans* LOH frequency following host association relative to the LOH frequency of *C. albicans* no host control for N2 (wildtype, grey, n = 8), *sek-1* (green, n = 9), and *bli-3* (blue, n = 8). **C)** Bloodstream *C. albicans* LOH frequency following host association relative to the LOH frequency of *C. albicans* no host control for N2 (grey, n = 11), *sek-1* (green, n =11), and *bli-3* (blue, n = 8). Plotted are the means and standard deviation (SD). Asterisks indicate significant differences (**** $p < 0.0001$, ** $p < 0.01$, ns = not significant; Kruskal-Wallis with post-hoc Dunn's multiple test).

Figure 2: *C. albicans cap1* Δ/Δ strain is more susceptible to *in vitro* and *in vivo* ROS
A) Plotted are the LOH frequencies of *C. albicans* exposed to 5mM H_2O_2 for 24 h relative to the frequencies of LOH of *C. albicans* without stress exposure. Plotted are the means and SD for both wildtype (WT) (grey, n = 12) and *cap1*Δ/Δ (orange, n = 19). Each data point represents an individual measurement. **B)** Plotted are the LOH frequencies of *C. albicans* exposed to each host environment relative to the no host frequency of LOH. Plotted are the means and SD. **C)** *C. albicans* LOH frequency following host exposure relative to the no host LOH frequency with 25 μM of alpha-lipoic acid (grey, N2: n = 9, *sek-1*: n = 9, *bli-3*: n = 9) and without 25 μM of alpha-lipoic acid (black, N2: n = 16, *sek-1*: n = 9, *bli-3*: n = 19). Each data point represents an individual measurement. Plotted are the means and SD. Asterisks indicate significant differences (**** $p < 0.0001$, *** $p < 0.005$, ** $p < 0.01$, * $p < 0.05$, ns = not significant; Mann-Whitney U test).

Figure 3: Genome-wide changes following host association
YMAPs of *C. albicans* following four-day exposure to N2 (WT), *sek-1*, and *bli-3* hosts with GAL1 LOH selection. Reference strain with the location of GAL1 on chromosome 1 indicated with a red line is displayed at the top. Y-axis on each chromosome indicates the chromosomal copy number. Chromosomal color indicates allelic ratio (grey = heterozygous, cyan/pink = homozygous, darker blue/purple = heterozygous with >2 alleles).

Figure 4: *C. albicans* evolves rapidly in immunocompetent hosts
A) Experimental schematic **B)** Time to 50% death for ten passages in healthy, immunocompetent (*glp-4*) hosts. Plotted are the mean (n = 6) and SD for each passage infected with *C. albicans*. **C)** Time to 50% for ten passages in immunocompromised (*glp-4; sek-1*) hosts infected with *C. albicans*. Plotted are the mean (n =6) and SD for each passage. Asterisks represent significant differences compared to the initial (P0) time point (**** $p < 0.0001$, *** $p < 0.005$, ** $p < 0.01$, * $p < 0.05$, Kruskal-Wallis with post-hoc Dunn's multiple test). **D)** Time to 50% death for immunocompetent and

706 immunocompromised hosts infected with *C. albicans* from the initial passage (Host P0),
707 *C. albicans* evolved for ten generations in the absence of hosts (No host P10), and *C.*
708 *albicans* evolved in the host environment for ten generations (Host P10). Asterisks
709 represent significant differences compared to the initial (P0) time point (*** $p < 0.005$, ns
710 = not significant, Kruskal-Wallis with post-hoc Dunn's multiple test).

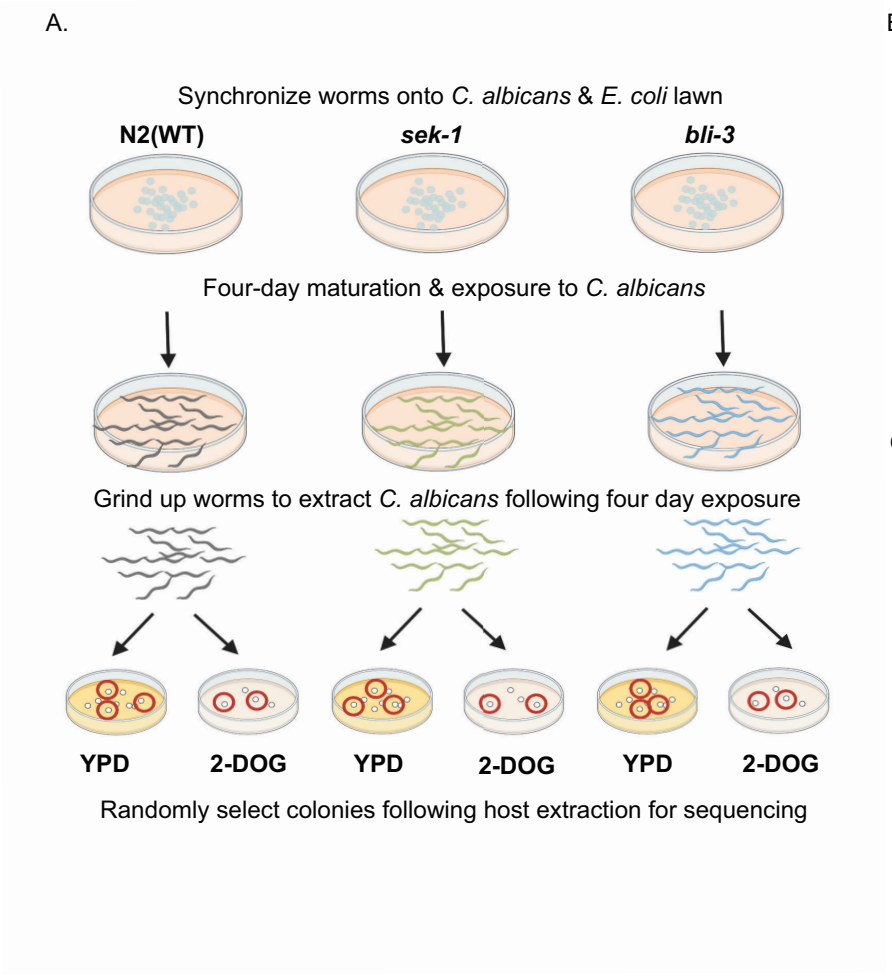

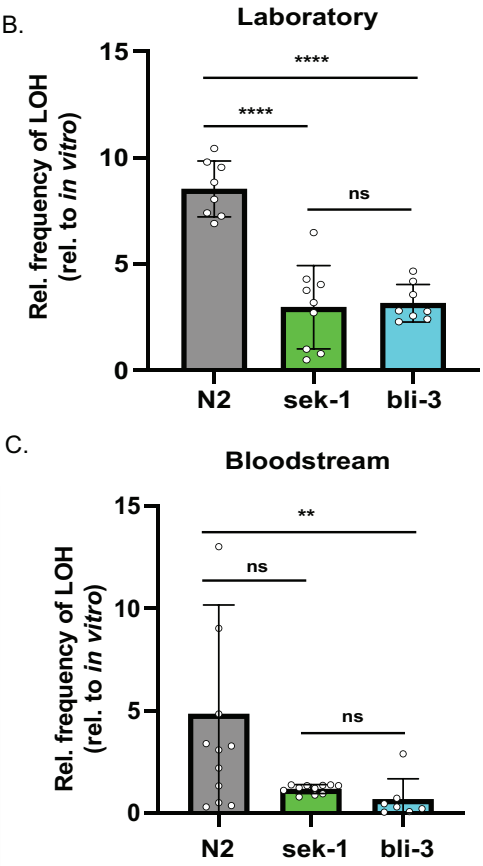

Infection and Immunity

IAI

Infection and Immunity

A.

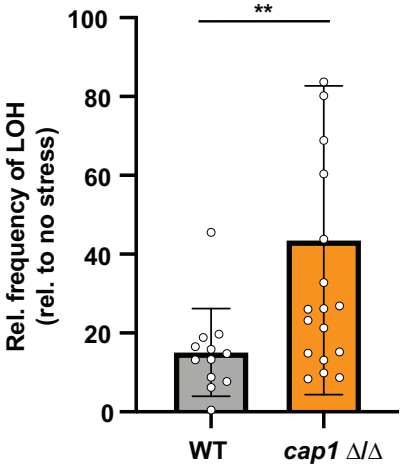

B.

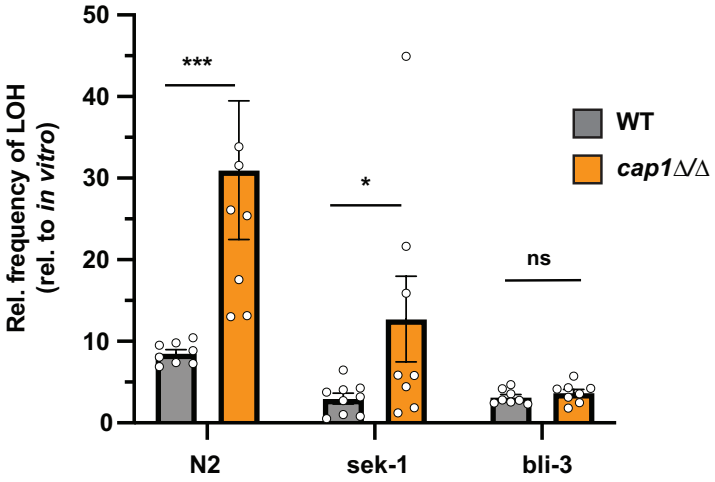

C.

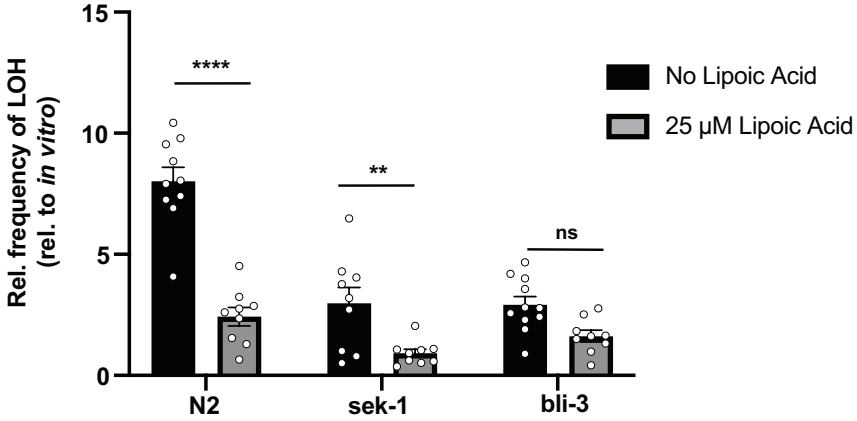

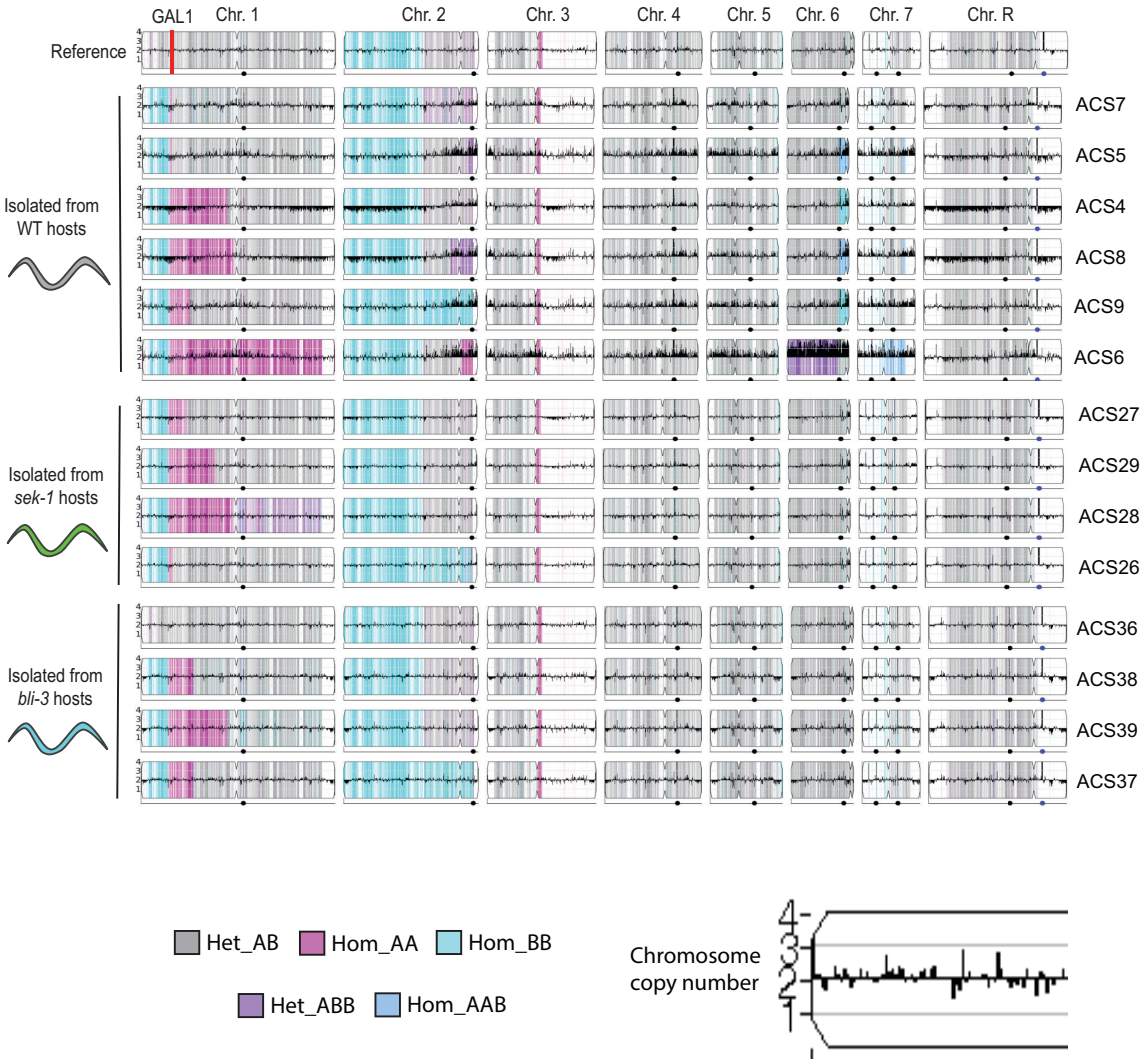

A.

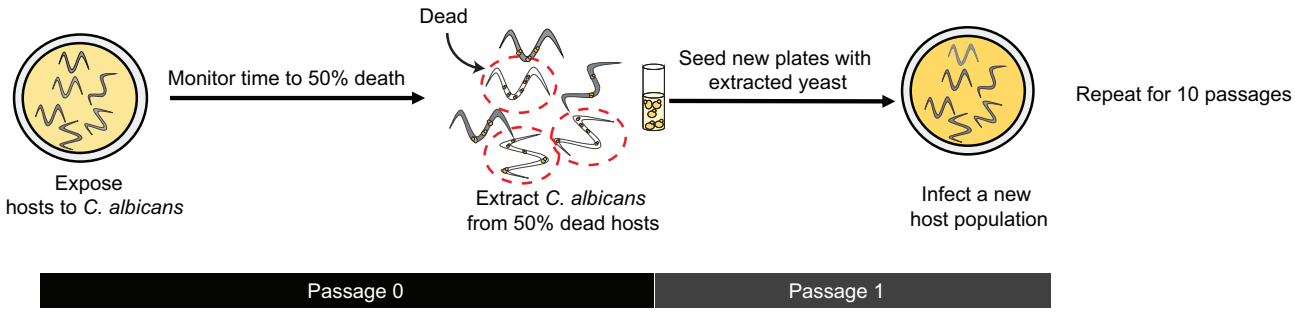

B.

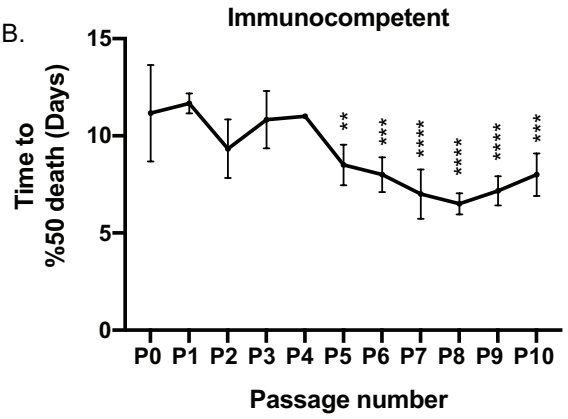

C.

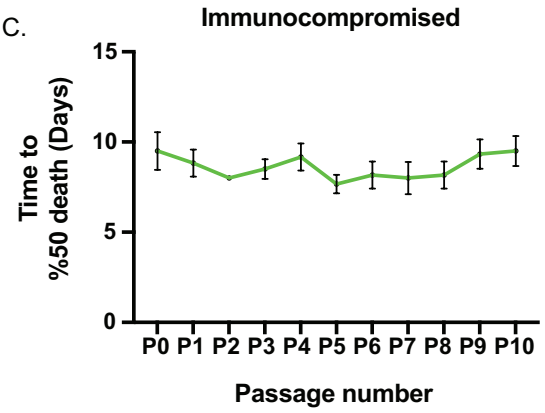

D.